JOURNAL OF GUIDANCE, CONTROL, AND DYNAMICS
Vol. 29, No. 1, January–February 2006

Optimal Fighter Pursuit–Evasion Maneuvers Found via Two-Sided Optimization

Kazuhiro Horie* and Bruce A. Conway†
University of Illinois at Urbana–Champaign, Urbana, Illinois 61801

An optimal pursuit–evasion fighter maneuver is formulated as a differential game and then solved by a recently developed numerical method, semidirect collocation with nonlinear programming. In this method, the optimal control for one player is found numerically, that is, by the optimizer, but that for the other player is based on the analytical necessary conditions of the problem. Because this requires costate variables for one player, the method is not a direct method. However, the problem can be placed in the form of conventional collocation with nonlinear programming. Thus, it is referred to it as a semidirect method. A genetic algorithm is used to provide an approximate solution, an initial guess, for the nonlinear programming problem solver. The method is applied to the challenging problem of optimal fighter aircraft pursuit–evasion in three dimensions. The obtained optimal trajectories are identified as having two phases: first a rapid change, primarily in direction, followed by a period of primarily vertical maneuvering. Solutions for various initial positions and velocities of the evader aircraft with respect to the pursuer are determined.

Introduction

OPTIMIZATION of air combat maneuvering, a type of flight-path optimization, involves finding the best flight path so that a fighter aircraft may overcome an opposing fighter aircraft. The obtained optimal path is useful for the evaluation of aircraft performance because the performance of a modern fighter aircraft in combat is determined dynamically. In addition, the requirements for the flight control system of a modern fighter aircraft are driven by the optimized flight path and control. Thus, optimization of air combat maneuvering is a potentially powerful aid for fighter aircraft development. Whereas flight-path optimization is presently done a priori, the development of a high-speed airborne computer in the future may enable real-time calculation of optimal air combat maneuvering.

In general, a flight-path optimization problem can be treated as a one-sided optimization problem (optimal control problem) or a two-sided optimization problem. The one-sided optimization problem considers only one player and has been successfully applied to a variety of applications for several decades. An example would be the minimization or maximization of a cost function for a single aircraft's flight path, for example, a minimum-time climb. However, a problem such as air combat is most accurately modeled using two competitive players. In that case, a path optimization problem often becomes a two-sided optimization called a zero-sum two-person differential game. A zero-sum two-person differential game mini–maximizes a cost function, which means that one of two competitive players minimizes a given cost function, whereas another maximizes the cost function. It was originally formulated by Isaacs[1]; Bryson and Ho[2] researched the same problem as an extension of an optimal control problem.

One important disadvantage of a one-sided optimization is that it cannot consider the optimal maneuvering of an opposing aircraft. Therefore, it is necessary to introduce a two-sided path optimization to solve the problem of air combat with an optimally maneuvering opponent. A variety of air combat problems modeled by a zero-sum two-person differential game have been solved analytically using simplified dynamics. One of the well-developed problems is the homicidal chauffeur problem, which is an analog to air combat between a low-speed, highly maneuverable evader and high-speed less-maneuverable pursuer. The problem was originally formulated by Isaacs[3] using aircraft models controlling only turn rate and without considering aerodynamic characteristics. Breakwell and Merz solved the problem in two-dimensional space with a limited turn rate for both aircraft.[4] One disadvantage of these analytical approaches is the quite simplified dynamics that must be assumed. A problem solved by Guelman et al.[5] is described using a model in which aerodynamic characteristics of the pursuer are considered but not those of the evader. This problem may represent the limit of the type of problems that may be solved analytically.

An answer to this disadvantage is to formulate a problem using realistic dynamics directly and solve it numerically. However, only a limited number of studies have been done using this approach because the optimization of a realistic air combat in which both fighter aircraft in battle maneuver optimally (using accurate aerodynamic characteristics) is very challenging to solve even numerically.

With regard to methods applied in recent two-sided problem solutions, Hillberg and Järmark[6] solved an air combat maneuvering problem in the horizontal plane with steady turn and realistic drag and thrust data. Järmark et al.[7] solved a qualitatively similar tail-chase air combat problem but used a very different method, differential dynamic programming, and considered only coplanar cases. A pursuit–evasion problem between missile and aircraft has been solved using an indirect, multiple shooting method by Breitner et al.[8,9] and by Lachner et al.[10] Raivio and Ehtamo[11] solved a pursuit–evasion problem for a visual identification of the target by iterating a direct method.

In this research, a new numerical method for zero-sum two-person differential games, the method of semidirect collocation with nonlinear programming (semi-DCNLP),[12] is applied to solve a pursuit–evasion game for three-dimensional air combat between a superior fighter and inferior fighter. The semi-DCNLP is developed employing DCNLP with the hope that it will share the robustness typically found for this method.

Two-Sided Optimization

In a zero-sum two-person differential game, two competitive sets of control variables, $\boldsymbol{u}_p$ and $\boldsymbol{u}_e$, drive a dynamic system. In this study, the equations of motion (1) and (2) for the states of the pursuer and evader, respectively, are considered:

$$\dot{\boldsymbol{x}}_p = \boldsymbol{f}_p(\boldsymbol{x}_p, \boldsymbol{u}_p, t) \tag{1}$$

Received 17 July 2003; revision received 24 March 2005; accepted for publication 24 March 2005.

*Graduate Research Assistant, Department of Aerospace Engineering.
†Professor, Department of Aerospace Engineering; bconway@uiuc.edu. Associate Fellow AIAA.

$$\dot{\boldsymbol{x}}_e = \boldsymbol{f}_e(\boldsymbol{x}_e, \boldsymbol{u}_e, t) \tag{2}$$

with initial conditions

$$\boldsymbol{x}_p(t_0) = \boldsymbol{x}_{p0} \tag{3}$$

$$\boldsymbol{x}_e(t_0) = \boldsymbol{x}_{e0} \tag{4}$$

Note that these equations of motion are often found in a pursuit–evasion game in fixed coordinates.

Terminal constraints, which are functions of the states at the final time and possibly of the final time, are

$$\boldsymbol{\psi}[\boldsymbol{x}_p(t_f), \boldsymbol{x}_e(t_f), t_f] = 0 \tag{5}$$

where t is time, t_0 is initial time, and t_f is the final time of the problem.

It is assumed that some control variables are bounded as

$$\boldsymbol{u}_{p,l} \le \boldsymbol{u}_p \le \boldsymbol{u}_{p,u} \tag{6}$$

$$\boldsymbol{u}_{e,l} \le \boldsymbol{u}_e \le \boldsymbol{u}_{e,u} \tag{7}$$

Path constraints are not considered in this research.

A problem of Mayer type is considered in this research. Then, the cost function for the problem is given as a function of the state variables and final time in the following form:

$$J(\boldsymbol{x}_p, \boldsymbol{x}_e, \boldsymbol{u}_p, \boldsymbol{u}_e, t) = \phi[\boldsymbol{x}_p(t_f), \boldsymbol{x}_e(t_f), t_f] \tag{8}$$

The feedback strategies, $\gamma_p$and γ_e, are introduced to determine the control variables, $\boldsymbol{u}_p$ and $\boldsymbol{u}_e$, as a function of state variables, that is, $\boldsymbol{u}_p(t) = \gamma_p(t, \boldsymbol{x}_p, \boldsymbol{x}_e)$ and $\boldsymbol{u}_e(t) = \gamma_e(t, \boldsymbol{x}_e, \boldsymbol{x}_p)$. When γ_p and γ_e are used, the value of the game, if it exists, is defined as

$$V = \min_{\gamma_p} \max_{\gamma_e} J = \max_{\gamma_e} \min_{\gamma_p} J \tag{9}$$

The existence of the value of the game is assumed in the following discussion.

The open-loop representation of the optimal feedback strategy, that is, the strategy along the optimal path as a function only of initial states, is defined as $\boldsymbol{u}_p^*(t) = \gamma_p(t, \boldsymbol{x}_{p0}, \boldsymbol{x}_{e0})$ and $\boldsymbol{u}_e^*(t) = \gamma_e(t, \boldsymbol{x}_{p0}, \boldsymbol{x}_{e0})$, which are considered to satisfy condition (9). Then, using initial states from Eqs. (3) and (4), the value of the game is expressed as

$$V = J\left(\boldsymbol{x}_p, \boldsymbol{x}_e, \boldsymbol{u}_p^*, \boldsymbol{u}_e^*, t\right) \tag{10}$$

A feedback saddle-point trajectory is obtained using an open-loop representation of the optimal feedback strategy, $\boldsymbol{u}_p^*$ and $\boldsymbol{u}_e^*$, under constraints (1–7).

Basar and Olsder[13] provide a set of necessary conditions for an open-loop representation of a feedback saddle-point trajectory. Here, the conditions are modified for system (1–7), a pursuit–evasion game in fixed coordinates. First, a Hamiltonian and a function of terminal conditions are introduced as

$$H = \boldsymbol{\lambda}_p^T \boldsymbol{f}_p + \boldsymbol{\lambda}_e^T \boldsymbol{f}_e \tag{11}$$

$$\Phi = \phi + \boldsymbol{\nu}^T \boldsymbol{\psi} \tag{12}$$

where $\boldsymbol{\lambda}_p$ and $\boldsymbol{\lambda}_e$ are adjoint variables and $\boldsymbol{\nu}$ is a set of Lagrange multipliers conjugate to the terminal constraints. Because the Hamiltonian is separable, the existence of the value of the game is assured.

When the Hamiltonian is used, adjoint equations are determined as

$$\dot{\boldsymbol{\lambda}}_p = -\left(\frac{\partial H}{\partial \boldsymbol{x}_p}\right)^T = -\left(\frac{\partial \boldsymbol{f}_p}{\partial \boldsymbol{x}_p}\right)^T \boldsymbol{\lambda}_p \tag{13}$$

$$\dot{\boldsymbol{\lambda}}_e = -\left(\frac{\partial H}{\partial \boldsymbol{x}_e}\right)^T = -\left(\frac{\partial \boldsymbol{f}_e}{\partial \boldsymbol{x}_e}\right)^T \boldsymbol{\lambda}_e \tag{14}$$

$$\boldsymbol{u}_p = \arg\min_{u_p} H = \arg\min_{u_p} \left(\boldsymbol{\lambda}_p^T \boldsymbol{f}_p\right) \tag{15}$$

$$\boldsymbol{u}_e = \arg\max_{u_e} H = \arg\max_{u_e} \left(\boldsymbol{\lambda}_e^T \boldsymbol{f}_e\right) \tag{16}$$

$$\boldsymbol{\lambda}_p(t_f) = \left(\frac{\partial \Phi}{\partial \boldsymbol{x}_p}\right)^T = \left(\frac{\partial \phi}{\partial \boldsymbol{x}_p} + \boldsymbol{\nu}^T \frac{\partial \boldsymbol{\psi}}{\partial \boldsymbol{x}_p}\right)^T \tag{17}$$

$$\boldsymbol{\lambda}_e(t_f) = \left(\frac{\partial \Phi}{\partial \boldsymbol{x}_e}\right)^T = \left(\frac{\partial \phi}{\partial \boldsymbol{x}_e} + \boldsymbol{\nu}^T \frac{\partial \boldsymbol{\psi}}{\partial \boldsymbol{x}_e}\right)^T \tag{18}$$

$$\left[H + \frac{\partial \Phi}{\partial t}\right]_{t=t_f} = 0 \tag{19}$$

Then, Equations (1), (2), (13), and (14) constitute a two-point boundary value problem (TPBVP) with the initial and terminal conditions (3–5) and (17–19) and controls satisfying bounds (6), (7), (15), and (16). However, it is normally very difficult to solve this TPBVP if the problem is large, that is, has many states and/or controls, or has strong nonlinearity, which often pertains for problems including realistic dynamics.

Many researchers have had success by using direct methods for the solution of such optimal control problems.[14–18] The DCNLP method[14,15,18] is such a direct method. In DCNLP, the continuous problem is discretized (in time). Implicit integration is used to enforce the system governing differential equations. Several types of implicit integration rules may be used, but in each case the rules yield nonlinear equations involving the discrete state and control parameters. There may be additional nonlinear and linear constraint equations involving the parameters, for example, expressing initial and terminal conditions. The problem is, thus, transformed into a nonlinear programming problem (NLP). The DCNLP method has been found to be very robust compared to indirect methods. There are several reasons for this. For one, when DCNLP is used, the problem is approximately half the size because there are no costate variables. For another, whereas an initial guess does need to be provided to the NLP problem solver, it is a guess only of the state and control history. The difficulty faced when using TPBVP solvers, of having to guess initial values of the nonintuitive Lagrange multipliers, is thus avoided.

Unfortunately the DCNLP method cannot be directly applied to a differential game or mini–max problem because the NLP solver on which the method relies must have just one objective function to minimize. However, a method we have developed, employing the structure of DCNLP, is capable of solving the differential game. The new method is constructed on the basis of the following concepts.

1) In DCNLP, control parameters are usually chosen by an optimizer such as NPSOL, that is, the analytical optimality conditions (or Pontryagin's principle) are not required, and hence, the system adjoint variables are not required. This is always applicable to the one-sided optimization problem.

2) If the adjoint variables for one player, for example, the pursuer, in a two-sided optimization are included in the DCNLP, then the control variables for the pursuer can be found from optimality condition (15). Because direct methods eschew the adjoint variables, we term this method semidirect or semi-DCNLP.

3) The optimal control variables for another player, for example, the evader, can be found numerically by the optimizer, to minimize the objective function just for the evader.

The method is expected to maintain the robust characteristics of DCNLP solutions. In this method, the optimality condition (15), associated adjoint equations (13), and terminal boundary conditions are incorporated into the DCNLP formulation. The terminal boundary conditions become

$$\boldsymbol{\psi}_{\text{ext}}(\boldsymbol{x}_p, \boldsymbol{x}_e, \boldsymbol{\lambda}_p, t_f) = 0 \tag{20}$$

These are boundary conditions derived from condition (17) that are not a function of $\boldsymbol{\lambda}_e$ or $\boldsymbol{\nu}$.

The control $\boldsymbol{u}_p$ for one of the players, obtained from condition (15), minimizes the cost function. Then, the original problem can be converted to

$$V = \max_{u_e} J \quad \text{subject to conditions (1–7), (13), (15), and (20)} \tag{21}$$

The problem represented by problem (21) can be used to construct a NLP problem, which can be solved using DCNLP, because now a (single) cost function is maximized and the constraints consist of differential equations and algebraic equations.

An extended Hamiltonian system (22) and (23) is considered to evaluate the characteristics of the solution of system (21),

$$H_{\text{ext}} = \boldsymbol{\lambda}_{Ep}^T \boldsymbol{f}_p + \boldsymbol{\lambda}_{Ee}^T \boldsymbol{f}_e + \boldsymbol{\lambda}_{E\lambda_p}^T \left(-\left(\frac{\partial \boldsymbol{f}_p}{\partial \boldsymbol{x}_p} \right)^T \boldsymbol{\lambda}_p \right)$$

$$= \boldsymbol{\lambda}_{Ep}^T \boldsymbol{f}_p + \boldsymbol{\lambda}_{Ee}^T \boldsymbol{f}_e - \boldsymbol{\lambda}_{E\lambda_p}^T \left(\frac{\partial \boldsymbol{f}_p}{\partial \boldsymbol{x}_p} \right)^T \boldsymbol{\lambda}_p \tag{22}$$

$$\Phi_{\text{ext}} = \phi(\boldsymbol{x}_p, \boldsymbol{x}_e, t_f) + \boldsymbol{\nu}_{E_1}^T \psi + \boldsymbol{\nu}_{E_2}^T \psi_{\text{ext}} \tag{23}$$

By applying the calculus of variations and Pontryagin principle, we have shown[12] that the solution of system (21) is satisfied with the necessary conditions for an open-loop representation of the feedback saddle-point trajectory when the conditions

$$\boldsymbol{\lambda}_{E_p} = \boldsymbol{\lambda}_p \tag{24}$$

$$\boldsymbol{\nu}_{E_2} = \boldsymbol{0} \tag{25}$$

hold. This is also consistent with the result in Papavassilopoulos and Cruz.[19]

The multipliers $\boldsymbol{\lambda}_{Ep}$ and $\boldsymbol{\nu}_{E2}$ can be obtained from the output of NPSOL or whichever NLP problem solver is used for the DCNLP-based method. Then, whether a DCNLP-based method provides the solution satisfying the necessary conditions may be determined by checking satisfaction of conditions (24) and (25).

Problem Definition

In this research, we will consider realistic air combat using the new numerical solver, the semi-DCNLP. This research focuses on the case of air combat between a superior fighter aircraft and an inferior fighter aircraft. A superior fighter, which has high-angle-of-attack (AOA) flight capability and thrust power with an afterburner, will attack an inferior fighter, which has conventional AOA flight capability and thrust power without afterburner.

Completion of the maneuver occurs when the superior fighter takes a shooting position on the inferior fighter. The superior fighter intends to minimize time of the completion of the maneuver, t_f, whereas the inferior fighter tries to maximize it. The air combat problem is, thus, a pursuit–evasion problem, a type of differential game, in which the cost function of the game is the time of completion. When fighters of such disparate capability are matched, a finite time of completion is guaranteed.

A three-degree-of-freedom, point-mass model is used to describe the aircraft trajectories. The trajectories of the aircraft are represented using six variables: velocity v, flight-path angle γ, heading angle ψ, down range x, cross range y, and altitude h. Angle of attack α and bank angle ϕ are used for the control of the fighter aircraft. The equations of motion are

$$\frac{\mathrm{d}v_i}{\mathrm{d}t} = \frac{1}{m_i}(T_i \cos\alpha_i - D_i) - g \sin\gamma_i \tag{26}$$

$$\frac{\mathrm{d}\gamma_i}{\mathrm{d}t} = \frac{1}{m_i v_i}(T_i \sin\alpha_i + L_i)\cos\phi_i - \frac{g}{v_i}\cos\gamma_i \tag{27}$$

$$\frac{\mathrm{d}\psi_i}{\mathrm{d}t} = \frac{1}{m_i v_i \cos\gamma_i}(T_i \sin\alpha_i + L_i)\sin\phi_i \tag{28}$$

$$\frac{\mathrm{d}x_i}{\mathrm{d}t} = v_i \cos\gamma_i \cos\psi_i \tag{29}$$

$$\frac{\mathrm{d}y_i}{\mathrm{d}t} = v_i \cos\gamma_i \sin\psi_i \tag{30}$$

$$\frac{\mathrm{d}h_i}{\mathrm{d}t} = v_i \sin\gamma_i \tag{31}$$

The subscript i indicates a superior fighter aircraft (the pursuer) when $i = p$ and an inferior fighter aircraft (the evader) when $i = e$. The lift force L and the drag force D are defined as

$$L_i = \tfrac{1}{2}\rho(h_i) v_i^2 S_i C_L(\alpha_i) \tag{32}$$

$$D_i = \tfrac{1}{2}\rho(h_i) v_i^2 S_i C_D(\alpha_i) \tag{33}$$

The gravitational acceleration g (=32.174 ft/s^2) and the wing area S (=300.0 ft^2) are constant. The model for atmospheric density ρ will be described, with density at sea level $\rho_s = 1.7556 \times 10^{-3}$ slug/ft^3, as[20]

$$\rho(h_i) = \rho_s[1 - 0.00688(h_i/1000)]^{4.256} \tag{34}$$

In this research, both fighter aircraft are modeled on the F-16A. Aerodynamic characteristics of the F-16A using the result of wind-tunnel testing[21] are approximated as

$$C_L = \begin{cases} 0.0174 + 4.3329\alpha - 1.3048\alpha^2 \\ \quad + 2.2442\alpha^3 - 5.8517\alpha^4 & (0 \le \alpha \le \pi/6) \\ -1.3106 + 10.7892\alpha - 9.2317\alpha^2 \\ \quad - 1.1194\alpha^3 + 2.1793\alpha^4 & (\pi/6 \le \alpha \le \pi/3) \\ 24.6577 - 71.0446\alpha + 83.1234\alpha^2 \\ \quad - 44.0862\alpha^3 + 8.6582\alpha^4 & (\pi/3 \le \alpha \le \pi/2) \end{cases} \tag{35}$$

$$C_D = \begin{cases} 0.0476 - 0.1462\alpha + 0.0491\alpha^2 \\ \quad + 12.8046\alpha^3 - 12.6985\alpha^4 & (0 \le \alpha \le \pi/6) \\ 0.5395 - 5.7972\alpha - 21.6625\alpha^2 \\ \quad + 21.6213\alpha^3 + 7.0364\alpha^4 & (\pi/6 \le \alpha \le \pi/3) \\ 16.6957 - 52.5918\alpha + 67.3227\alpha^2 \\ \quad - 37.086\alpha^3 + 7.4807\alpha^4 & (\pi/3 \le \alpha \le \pi/2) \end{cases} \tag{36}$$

Angles of attack are constrained in this research for pursuer and for evader, that is,

$$0 \le \alpha_p \le \pi/2 \tag{37}$$

$$0 \le \alpha_e \le \pi/6 \tag{38}$$

The thrust is established on the basis of the actual F-16A aircraft at 0.5 Mach and 20,000-ft altitude, with afterburner for the pursuer, yielding $T_p = 12,274$ lb, and without afterburner for the evader, yielding $T_e = 6124$ lb (Ref. 21). Of course, the real engine has performance that cannot be represented by a simple function of Mach number and altitude. Therefore, the given fixed values are applied to simplify the solution of the numerical optimization. The mass of the aircraft, m(=637.16 slug), is set as constant because the air combat time is generally brief.

A terminal condition is required to solve the air combat problem as a pursuit–evasion problem. In the real world, many fighter aircraft have a rear-aspect short-range missile and/or gun for attack. Thus, tail chasing is one of the traditional tactics of air combat.[7] Tail chasing is used as a proper terminal condition and modeled as an interception condition with the same heading angle,

$$x_p(t_f) = x_e(t_f) \tag{39}$$

$$y_p(t_f) = y_e(t_f) \tag{40}$$

$$h_p(t_f) = h_e(t_f) \tag{41}$$

$$\psi_p(t_f) = \psi_e(t_f) \tag{42}$$

The problem is characterized as a two-sided flight-path optimization problem,

$$V = \min_{\alpha_p,\phi_p}\max_{\alpha_e,\phi_e} t_f \tag{43}$$

subject to conditions (26–31) and (39–42) for given initial conditions.

The semi-DCNLP method is applied to solve the problem. Therefore, the adjoint equations and the optimality conditions for the superior fighter aircraft (the pursuer) are required. The Hamiltonian for the problem is

$$\begin{aligned} H = {} & \left(\lambda_{v_p}/m_p\right)[(T_p\cos\alpha_p - D_p) - m_p g\sin\gamma_p] \\ & + \left(\lambda_{\gamma_p}/m_p v_p\right)[(T_p\sin\alpha_p + L_p)\cos\phi_p - m_p g\cos\gamma_p] \\ & + \left(\lambda_{\psi_p}/m_p v_p\cos\gamma_p\right)(T_p\sin\alpha_p + L_p)\sin\phi_p \\ & + \lambda_{x_p} v_p\cos\gamma_p\cos\psi_p \\ & + \lambda_{y_p} v_p\cos\gamma_p\sin\psi_p + \lambda_{h_p} v_p\sin\gamma_p + H_e \end{aligned} \tag{44}$$

where H_e indicates a part of the Hamiltonian that depends on the evader.

When the Pontryagin principle is applied, the following adjoint equations are obtained:

$$\begin{aligned} \frac{\mathrm{d}\lambda_{v_p}}{\mathrm{d}t} = {} & \frac{2\lambda_{v_p} D_p}{m_p v_p} + \frac{\lambda_{\gamma_p}}{m_p v_p^2}[(T_p\sin\alpha_p - L_p)\cos\phi_p - m_p g\cos\gamma_p] \\ & + \frac{\lambda_{\psi_p}}{m_p v_p^2\cos\gamma_p}(T_p\sin\alpha_p - L_p)\sin\phi_p - \lambda_{x_p}\cos\gamma_p\cos\psi_p \\ & - \lambda_{y_p}\cos\gamma_p\sin\psi_p - \lambda_{h_p}\sin\gamma_p \end{aligned} \tag{45}$$

$$\begin{aligned} \frac{\mathrm{d}\lambda_{\gamma_p}}{\mathrm{d}t} = {} & \lambda_{v_p} g\cos\gamma_p - \frac{\lambda_{\gamma_p} g\sin\gamma_p}{v_p} - \frac{\lambda_{\psi_p}\tan\gamma_p}{m_p v_p\cos\gamma_p} \\ & \times (T_p\sin\alpha_p + L_p)\sin\phi_p + \lambda_{x_p} v_p\sin\gamma_p\cos\psi_p \\ & + \lambda_{y_p} v_p\sin\gamma_p\sin\psi_p - \lambda_{h_p} v_p\cos\gamma_p \end{aligned} \tag{46}$$

$$\frac{\mathrm{d}\lambda_{\psi_p}}{\mathrm{d}t} = \lambda_{x_p} v_p\cos\gamma_p\sin\psi_p - \lambda_{y_p} v_p\cos\gamma_p\cos\psi_p \tag{47}$$

$$\frac{\mathrm{d}\lambda_{x_p}}{\mathrm{d}t} = 0 \tag{48}$$

$$\frac{\mathrm{d}\lambda_{y_p}}{\mathrm{d}t} = 0 \tag{49}$$

$$\frac{\mathrm{d}\lambda_{h_p}}{\mathrm{d}t} = \frac{1}{m_p\rho(h_p)}\left\{\lambda_{v_p} D_p - \frac{\lambda_{\gamma_p} L_p\cos\phi_p}{v_p} - \frac{\lambda_{\psi_p} L_p\sin\phi_p}{v_p\cos\gamma_p}\right\}\frac{\mathrm{d}\rho}{\mathrm{d}h_p} \tag{50}$$

Equation (48) indicates that λ_{xp} is constant. Then it is convenient to scale the remaining adjoint variables by λ_{xp}, thus removing λ_{xp} explicitly from the problem. The scaled adjoint variables are indicated with a superscript #, and then the adjoint equations (45–50) are rewritten as follows:

$$\begin{aligned} \frac{\mathrm{d}\lambda^{\#}_{vp}}{\mathrm{d}t} = {} & \frac{2\lambda^{\#}_{vp} D_p}{m_p v_p} + \frac{\lambda^{\#}_{\gamma p}}{m_p v_p^2}\{(T_p\sin\alpha_p - L_p)\cos\phi_p - m_p g\cos\gamma_p\} \\ & + \frac{\lambda^{\#}_{\psi p}}{m_p v_p^2\cos\gamma_p}(T_p\sin\alpha_p - L_p)\sin\phi_p - \cos\gamma_p\cos\psi_p \\ & - \lambda^{\#}_{yp}\cos\gamma_p\sin\psi_p - \lambda^{\#}_{hp}\sin\gamma_p \end{aligned} \tag{51}$$

$$\begin{aligned} \frac{\mathrm{d}\lambda^{\#}_{\gamma p}}{\mathrm{d}t} = {} & \lambda^{\#}_{vp} g\cos\gamma_p - \frac{\lambda^{\#}_{\gamma p} g\sin\gamma_p}{v_p} - \frac{\lambda^{\#}_{\psi p}\tan\gamma_p}{m_p v_p\cos\gamma_p} \\ & \times (T_p\sin\alpha_p + L_p)\sin\phi_p + v_p\sin\gamma_p\cos\psi_p \\ & + \lambda^{\#}_{yp} v_p\sin\gamma_p\sin\psi_p - \lambda^{\#}_{hp} v_p\cos\gamma_p \end{aligned} \tag{52}$$

$$\frac{\mathrm{d}\lambda^{\#}_{\psi p}}{\mathrm{d}t} = v_p\cos\gamma_p\sin\psi_p - \lambda^{\#}_{yp} v_p\cos\gamma_p\cos\psi_p \tag{53}$$

$$\frac{\mathrm{d}\lambda^{\#}_{yp}}{\mathrm{d}t} = 0 \tag{54}$$

$$\frac{\mathrm{d}\lambda^{\#}_{hp}}{\mathrm{d}t} = \frac{1}{m_p\rho(h_p)}\left(\lambda^{\#}_{vp} D_p - \frac{\lambda^{\#}_{\gamma p} L_p\cos\phi_p}{v_p} - \frac{\lambda^{\#}_{\psi p} L_p\sin\phi_p}{v_p\cos\gamma_p}\right)\frac{\mathrm{d}\rho}{\mathrm{d}h_p} \tag{55}$$

A bounded AOA for the pursuer is transformed into a new unbounded variable using the relation

$$\alpha_p = (\pi/4)(1 - \cos\tau_{\alpha p}) \tag{56}$$

Then the first-order optimality conditions become

$$\begin{aligned} H_{\tau_{\alpha_p}} = {} & \frac{\pi}{4}\sin\tau_{\alpha p}\left\{\frac{\lambda^{\#}_{vp}}{m_p}\left(-T_p\sin\alpha_p - \frac{D_p}{C_D(\alpha)}\frac{\mathrm{d}C_D}{\mathrm{d}\alpha}\right)\right. \\ & + \frac{\lambda^{\#}_{\gamma p}}{m_p v_p}\left(T_p\cos\alpha_p + \frac{L_p}{C_L(\alpha)}\frac{\mathrm{d}C_L}{\mathrm{d}\alpha}\right)\cos\phi_p \\ & \left. + \frac{\lambda^{\#}_{\psi p}}{m_p v_p\cos\gamma_p}\left(T_p\cos\alpha_p + \frac{L_p}{C_L(\alpha)}\frac{\mathrm{d}C_L}{\mathrm{d}\alpha}\right)\sin\phi_p\right\} = 0 \end{aligned} \tag{57}$$

$$\begin{aligned} H_{\phi_p} = {} & -\frac{\lambda^{\#}_{\gamma p}}{m_p v_p}(T_p\sin\alpha_p + L_p)\sin\phi_p \\ & + \frac{\lambda^{\#}_{\psi p}}{m_p v_p\cos\gamma_p}(T_p\sin\alpha_p + L_p)\cos\phi_p = 0 \end{aligned} \tag{58}$$

The boundary conditions corresponding to the adjoint equations are obtained through the following process: Let

$$\begin{aligned} \Phi = {} & -t_f + \nu_1(x_p - x_e) + \nu_2(y_p - y_e) \\ & + \nu_3(z_p - z_e) + \nu_4(\psi_p - \psi_e)|_{t=t_f} \end{aligned} \tag{59}$$

then the terminal boundary conditions on the adjoint variables become

$$\lambda_{x_p}(t_f) = \left.\frac{\partial\Phi}{\partial x_p}\right|_{t=t_f} = \nu_1 \tag{60}$$

$$\lambda^{\#}_{vp}(t_f) = \frac{1}{\lambda_{x_p}(t_f)}\left.\frac{\partial\Phi}{\partial v_p}\right|_{t=t_f} = 0 \tag{61}$$

$$\lambda^{\#}_{\gamma p}(t_f) = \frac{1}{\lambda_{x_p}(t_f)}\left.\frac{\partial\Phi}{\partial\gamma_p}\right|_{t=t_f} = 0 \tag{62}$$

$$\lambda^{\#}_{\psi p}(t_f) = \frac{1}{\lambda_{x_p}(t_f)}\left.\frac{\partial\Phi}{\partial\psi_p}\right|_{t=t_f} = \frac{\nu_4}{\nu_1} \tag{63}$$

$$\lambda^{\#}_{yp}(t_f) = \frac{1}{\lambda_{x_p}(t_f)}\left.\frac{\partial\Phi}{\partial y_p}\right|_{t=t_f} = \frac{\nu_2}{\nu_1} \tag{64}$$

$$\lambda^{\#}_{hp}(t_f) = \frac{1}{\lambda_{x_p}(t_f)}\left.\frac{\partial\Phi}{\partial h_p}\right|_{t=t_f} = \frac{\nu_3}{\nu_1} \tag{65}$$

Note that, of the boundary conditions on the adjoint variables in the semi-DCNLP problem, only conditions (61) and (62) are applied because ν_1, ν_2, ν_3, and ν_4 are unknown parameters.

The semi-DCNLP formulation of the air combat problem is, thus,

$$J = \max_{\gamma_e, \psi_e} t_f \tag{66}$$

subject to Eqs. (26–31) and (51–55) as differential equations, conditions (39–42) and (61) and (62) as terminal conditions, and constraints (57) and (58) as algebraic constraints, for given initial conditions.

Results

To make the air combat problem realistic, we choose initial conditions representative of real air combat, and to make the problem interesting, the aircraft need altitude to allow them to maneuver. In this research, 20,000-ft altitude and 400-ft/s velocity are selected as a nominal, initial condition for both aircraft. To evaluate three-dimensional pursuit–evasion maneuvering, the relative initial position and relative motion between the pursuer and the evader are given out-of-plane components. The nominal initial condition is that 1) the evader flies on the right side of the pursuer at a line of sight 30 deg from forward, 2) both aircraft fly in the same direction, 3) both aircraft are in level flight, and 4) the distance between the pursuer and the evader is 4000 ft.

The state variables and the time are normalized by a reference time of 10.0 s, a reference length of 4000 ft, and a reference mass of 637.16 slug, as appropriate. Normalization avoids reducing the accuracy of the variables by keeping them to similar order and improves the robustness of the NLP problem solver.

The pursuer is put at the origin of the coordinate system at the initial time. Thus, the initial condition for the nominal case is

$$\begin{aligned}[v_p, \gamma_p, \psi_p, x_p, y_p, h_p, v_e, \gamma_e, \psi_e, x_e, y_e, h_e] \\ = [1.0, 0.0, 0.0, 0.0, 0.0, 5.0, 1.0, 0.0, 0.0, \\ \cos(-\pi/6), \sin(-\pi/6), 5.0]\end{aligned} \tag{67}$$

The semi-DCNLP problem has been solved using a discretization of the problem based on the work of Herman and Conway, in which fifth-degree polynomials are used to represent the state variables in each segment of the problem.[15] An initial guess of the discrete solution of the problem is required by the NLP problem solver. For this purpose, an approximate solution of the problem is obtained using a method developed by Horie and Conway based on genetic algorithms (GAs).[22] Ordinarily, as mentioned before, the DCNLP method is quite robust, and a sufficient initial guess, of the state and control variable time histories, is not difficult to arrive at. However, the semi-DCNLP requires in addition an initial guess of the costates for one player; these are not intuitive, even their magnitudes are difficult to guess a priori. An approximate solution for the optimal trajectories and for the costate time histories, using a GA, can be found from a random population of initial guesses of the GA chromosome; it is an effective way to generate an initial guess for the NLP solver from which the solver can converge.

With this guess, the NLP solver converges to an optimal solution, that is all of the system governing equations (26–31) and (51–55) are satisfied implicitly using the fifth-degree Gauss–Lobatto (G–L) collocation rules (Ref. 15) and the constraints (39–42), (57) and (58), and (61) and (62) are satisfied to $\mathcal{O}(10^{-7})$, for the given initial conditions, whereas the time to interception (66) is maximized. The NLP problem solver, NZSOL, outputs the Kuhn–Tucker (K–T) multipliers conjugate to the constraints. However, we have previously shown[16,23,24] that when the G–L implicit integration rules are used the K–T multipliers are (except perhaps for a multiplicative constant) a discrete representation of the continuous Lagrange multipliers of the problem. By inspection of the multipliers, we note that in the converged solution the adjoint variables constituting the left-hand side of Eq. (24) are very close numerically to the corresponding Lagrange multipliers from the right side of Eq. (24). In addition, condition (25) is satisfied by the solution.

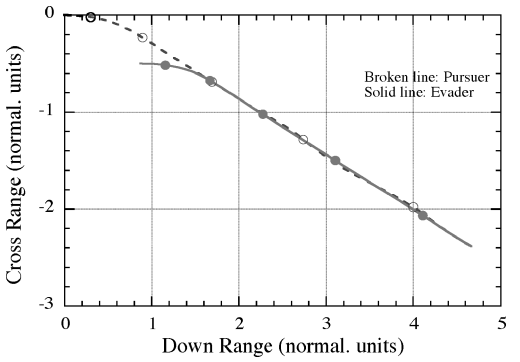

Fig. 1 Saddle-point trajectories on a horizontal plane (nominal case).

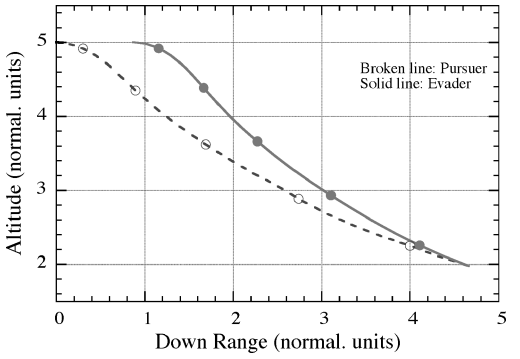

Fig. 2 Saddle-point trajectories on a vertical (*X*–*Z*) plane (nominal case).

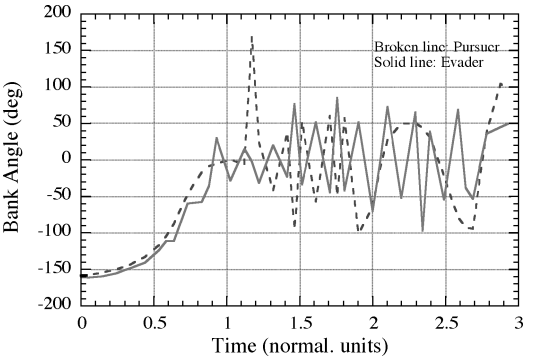

Fig. 3 Histories of bank angle of saddle-point trajectories (nominal case).

The following observations are made from the solutions.

1) The trajectories (Figs. 1 and 2) show the three-dimensional realistic air combat problem (pursuit–evasion problem) has two phases, qualitatively speaking. In the first phase, the aircraft are steered in three-dimensional space so that their maneuvers will be primarily in a vertical plane in a second phase. In the second phase, the aircraft mainly do dive maneuvers in a vertical plane. These characteristics of the two phases are observed in Figs. 3–6. In Figs. 3–6, the characters of the time histories change at approximately 0.9 time units (9 s). These characteristics are qualitatively observed in simpler problems such as the homicidal chauffeur problem, which has a similar two-phase structure.[3]

2) The bank angle in the second phase shows chattering control (Fig. 3). This is supported by the fact that $\lambda^{\#}_{\gamma p}$ and $\lambda^{\#}_{\psi p}$ become zero in this region and, thus, Eq. (58) cannot determine the bank angle, that is, the solution for the bank angle is singular. From the system equations (26–31), it is clear that the principal effect of the nonzero bank angle ϕ is to produce a nonzero time rate of change the heading angle ψ. However, one can see, for example, in Fig. 7, that $\dot{\psi}$ changes rapidly at the beginning but becomes zero as the aircraft

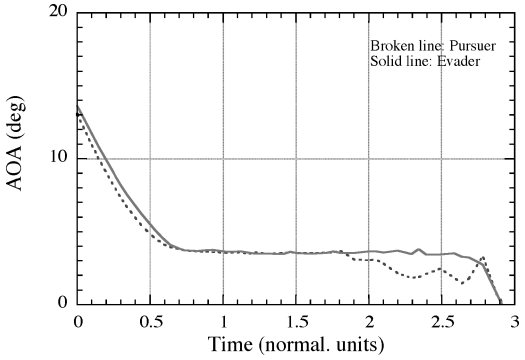

Fig. 4 Histories of angle of attack of saddle-point trajectories (nominal case).

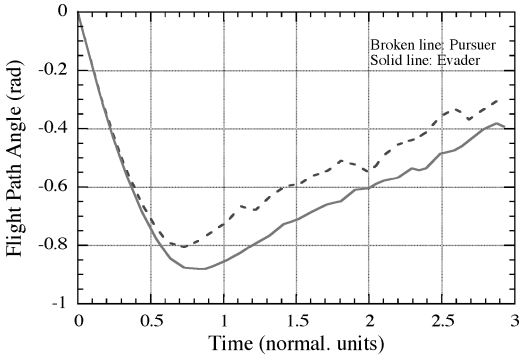

Fig. 5 Histories of flight-path angle of saddle-point trajectories (nominal case).

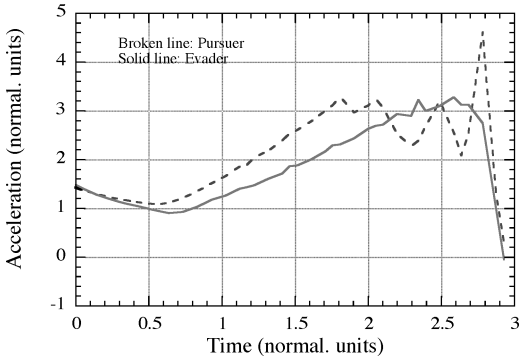

Fig. 6 Histories of normal acceleration of saddle-point trajectories (nominal case).

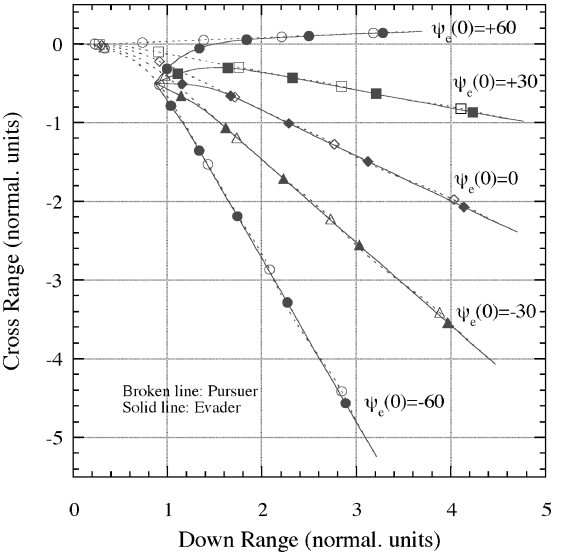

Fig. 7 Saddle-point trajectories on horizontal plane: parameter, initial heading angle of evader.

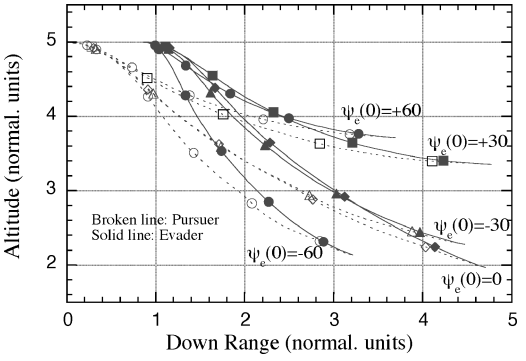

Fig. 8 Saddle-point trajectories on vertical (*X–Z*) plane: parameter, initial heading angle of evader.

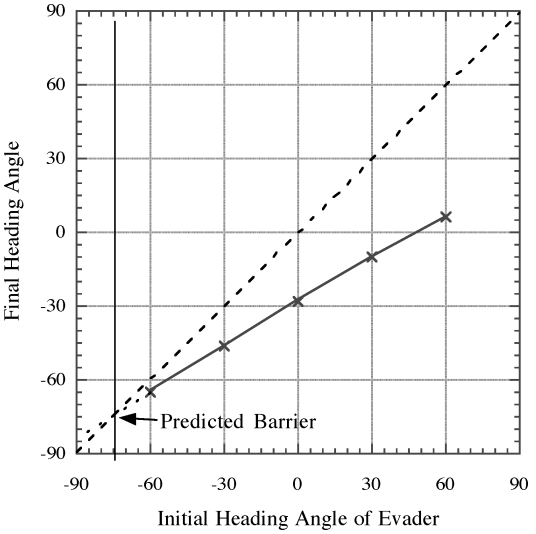

Fig. 9 Evader initial heading angle vs final heading angle.

take fixed headings for the pursuit. That is, the chattering bank angle in the second phase is likely a numerical artifact; the value should probably be zero. Except for this observation, the bank angle control is consistent with Figs. 1 and 2, that is, the aircraft takes a bank angle in the first phase but does not in the second phase.

3) Figure 6 shows that the aircraft uses feasible vertical maneuvering, that is, it maneuvers at rates tolerable by a human pilot. The normal acceleration ranges from 1 *g* through 5 *g* throughout the time history. Also, the angle of attack is below 15 deg. This means that the pursuer does not use poststall flight capability in this case.

To evaluate the effect of relative motion, the initial heading angle of the evader is varied while maintaining the same initial conditions as in the nominal case for the other parameters. The semi-DCNLP method yields convergent solutions for cases in which the heading angle of the evader ranges from −60 to +60 deg of the initial heading angle of the pursuer.

Figures 7 and 8 show the group of saddle-point trajectories. All of the trajectories obtained are qualitatively the same as that of the nominal case (in which the initial heading angle of the evader is zero). Also, the smaller the initial heading angle is, the smaller the total change of the heading angle. This tendency is recognized in Fig. 9, which shows the relationship between the initial and the final heading angle of the evader. Figure 9 shows the relationship is linear and predicts that the initial angle is equal to the final angle when the initial angle is approximately 75 deg. It is predicted that the evader's maneuver changes qualitatively beyond this point, otherwise the magnitude of the initial heading angle of the evader would become

larger than the magnitude of the final heading angle, and in that case the evader would approach the pursuer.

To evaluate the effect of initial relative position, the initial line of sight (LOS) is varied while maintaining the same initial conditions as in the nominal case for the other parameters. The semi-DCNLP method yields convergent solutions for cases ranging from −30 to −90 deg of the initial LOS.

Figures 10 and 11 show a group of saddle-point trajectories. Figure 12 shows the relationship between the initial LOS and the final heading angle. Figures 10–12 suggest the interesting result that

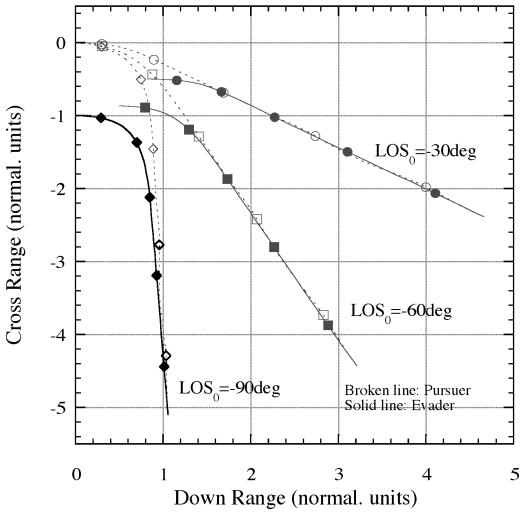

Fig. 10 Saddle-point trajectories on horizontal plane: parameter, initial LOS angle.

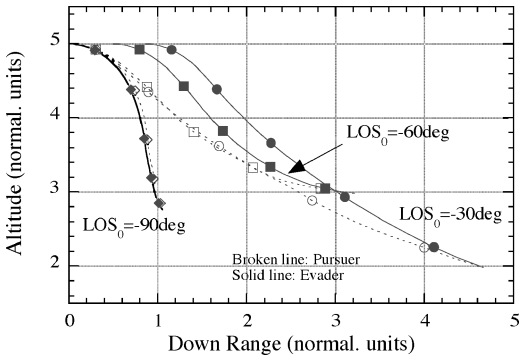

Fig. 11 Saddle-point trajectories on vertical (*X–Z*) plane: parameter, initial LOS angle.

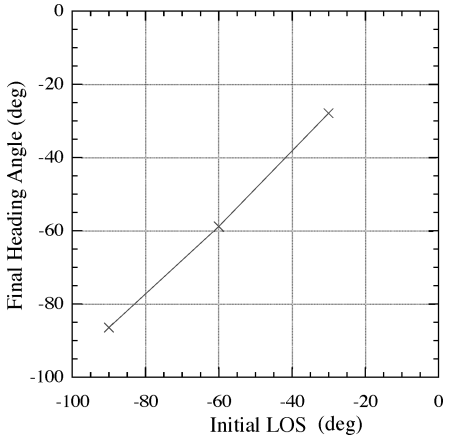

Fig. 12 Initial LOS vs final heading angle: parameter, initial LOS angle.

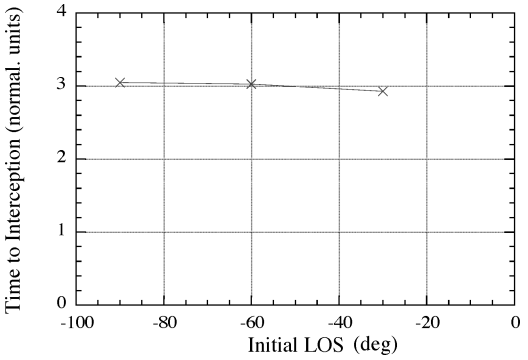

Fig. 13 Time to interception: parameter, initial LOS angle.

the initial LOS is close to the final heading angle. Figure 13 shows the relationship between the initial LOS and the time to interception, the objective function. It is observed from Fig. 13 that the initial LOS hardly affects the value of the time to interception.

Conclusions

An air combat problem with realistic aerodynamic and aircraft models, between a superior fighter and an inferior fighter, is modeled using a pursuit–evasion game approach and is solved using the semi-DCNLP method. Solutions of this problem are rarely seen in the literature because the problem is very complicated and difficult to solve using extant methods. However, the semi-DCNLP method, assisted with an initial guess obtained via a GA, solves the problem easily and robustly.

For three-dimensional air combat, we find that the optimal trajectory consists qualitatively of two phases. The aircraft first maneuver out of the original plane of their motion, followed by a second phase in which the motion is mainly confined to a vertical plane. It is also found that change in the initial LOS changes the value of the cost function, the time to capture, only slightly, whereas change in the initial heading angle and altitude of the evader change the value of the cost function significantly.

This research has identified some characteristics of pursuit–evasion type air combat using the semi-DCNLP method for trajectory optimization. Two suggestions are made for extensions of the research. The first is to use a more accurate model, for such things as thrust and atmospheric density, and then identify more precisely the characteristics of the air combat. This would be useful for the evaluation of the combat ability of a specific fighter aircraft. Another suggestion is to evaluate the qualitative differences in optimal air combat maneuvering among a variety of models and, thus, find the most cost-effective model. The idea is to conserve calculation time and provide the saddle-point trajectories in just sufficient quality. This is perhaps more useful for trade-off studies in the conceptual design phase of fighter aircraft.

References

[1]Isaacs, R., *Games of Pursuit*, Rept. P-257, Rand Corp., Santa Monica, CA, Nov. 1951.

[2]Bryson, A. E., and Ho, Y. C., *Applied Optimal Control*, Hemisphere, New York, 1975, pp. 271–293.

[3]Isaacs, R., *Differential Games*, Wiley, New York, 1965, pp. 278–280.

[4]Breakwell, J. V., and Merz, A. W., "Minimum Required Capture Radius in a Coplanar Model of the Aerial Combat Problem," *AIAA Journal*, Vol. 15, No. 8, 1977, pp. 1089–1094.

[5]Guelman, M., Shinar, J., and Green, A., "Qualitative Study of a Planar Pursuit Evasion Game in the Atmosphere," *Journal of Guidance, Control and Dynamics*, Vol. 13, No. 6, 1990, pp. 1136–1142.

[6]Hillberg, C., and Järmark, B., "Pursuit-Evasion Between Two Realistic Aircraft," *Journal of Guidance, Control, and Dynamics*, Vol. 7, No. 6, 1984, pp. 690–694.

[7]Järmark, B., Merz, A. W., and Breakwell, J. V., "The Variable Speed Tail-Chase Aerial Combat Problem," *Journal of Guidance, Control and Dynamics*, Vol. 4, No. 3, 1981, pp. 323–328.

[8]Breitner, M. H., Pesch, H. J., and Grimm, W., "Complex Differential Games of Pursuit–Evasion Type with State Constraints, Part 1: Necessary

Conditions for Open-Loop Strategies," *Journal of Optimization Theory and Applications*, Vol. 78, No. 3, 1993, pp. 419–441.

[9]Breitner, M. H., Pesch, H. J., and Grimm, W., "Complex Differential Games of Pursuit-Evasion Type with State Constraints, Part 2: Numerical Computation of Open-Loop Strategies," *Journal of Optimization Theory and Applications*, Vol. 78, No. 3, 1993, pp. 443–463.

[10]Lachner, R., Breitner, M. H., and Pesch, H. J., "Three-Dimensional Air Combat: Numerical Solution of Complex Differential Games," *Advances in Dynamic Games and Applications*, edited by G. J. Olsder, Birkhäuser, Boston, 1995, pp. 165–190.

[11]Raivio, T., and Ehtamo, H., "Visual Aircraft Identification as a Pursuit–Evasion Game," *Journal of Guidance, Control, and Dynamics*, Vol. 23, No. 4, 2000, pp. 701–708.

[12]Horie, K., "Collocation with Nonlinear Programming for Two-Sided Flight Path Optimization", Ph.D. Dissertation, Dept. of Aeronautical and Astronautical Engineering, Univ. of Illinois, Urbana, IL, Feb. 2002.

[13]Basar, T., and Olsder, G. J., *Dynamic Noncooperative Game Theory*, Society for Industrial and Applied Mathematics, Philadelphia, 1999, pp. 424–441.

[14]Hargraves, C. R., and Paris, S. W., "Direct Trajectory Optimization Using Nonlinear Programming and Collocation," *Journal of Guidance, Control and Dynamics*, Vol. 10, No. 4, 1987, pp. 338–342.

[15]Herman, A. L., and Conway, B. A., "Direct Optimization Using Collocation Based on High-Order Gauss–Lobatto Quadrature Rules," *Journal of Guidance, Control, and Dynamics*, Vol. 19, No. 3, 1996, pp. 592–599.

[16]Enright, P. J., and Conway, B. A., "Discrete Approximations to Optimal Trajectories Using Direct Transcription and Nonlinear Programming," *Journal of Guidance, Control, and Dynamics*, Vol. 15, No. 4, 1992, pp. 994–1002.

[17]Herman, A. L., and Conway, B. A., "Optimal Low-Thrust, Earth–Moon Orbit Transfer," *Journal of Guidance, Control, and Dynamics*, Vol. 21, No. 1, 1998, pp. 141–147.

[18]Betts, J. T., *Practical Methods for Optimal Control Using Nonlinear Programming,* Society for Industrial and Applied Mathematics, Philadelphia, 2001, pp. 61–125.

[19]Papavassilopoulos, G. P., and Cruz, J. B., Jr., "Nonclassical Control Problems and Stackelberg Games," *IEEE Transactions on Automatic Control*, Vol. AC-24, No. 2, 1979, pp. 155–166.

[20]McCormick, B. W., *Aerodynamics, Aeronautics and Flight Mechanics*, Wiley, New York, 1994, pp. 23–26.

[21]Gilbert, W. P., Nguyen, L. T., and Van Gunst, R. W., "Simulator Study of the Effectiveness of an Automatic Control System Designed to Improve the High-Angle-of-Attack Characteristics of a Fighter Airplane," NASA TN D-8176, Langley Research Center, 1976.

[22]Horie, K., and Conway, B. A., "GA Pre-Processing for Numerical Solution of Differential Games Problems," *Journal of Guidance, Control, and Dynamics*, Vol. 27, No. 6, 2004, pp. 1075–1078.

[23]Enright, P. J., "Optimal Finite-Thrust Spacecraft Trajectories Using Direct Transcription and Nonlinear Programming," Ph.D. Dissertation, Dept. of Aeronautical and Astronautical Engineering, Univ. of Illinois, Urbana, IL, Jan. 1991.

[24]Herman, A. L., "Improved Collocation Methods with Application to Direct Trajectory Optimization," Ph.D. Dissertation, Dept. of Aeronautical and Astronautical Engineering, Univ. of Illinois, Urbana, IL, Sept. 1995.